Design of a Gravity-Balanced General Spatial Serial-Type Manipulator[1]

Po-Yang Lin
Graduate Student
Department of Mechanical Engineering,
National Taiwan University,
Taipei 10617, Taiwan

Win-Bin Shieh
Assistant Professor
Department of Mechanical Engineering,
Mingchi University of Technology,
Taipei 24301, Taiwan

Dar-Zen Chen[2]
Professor
Department of Mechanical Engineering,
National Taiwan University,
Taipei 10617, Taiwan
e-mail: dzchen@ntu.edu.tw

A novel methodology for the design of a gravity-balanced serial-type spatial manipulator is presented. In the design, gravity effects of the system can be completely compensated at any configuration. The gravity balance of the n-DOF manipulator is achieved by the suspensions of only n zero-free-length springs, where each spring is individually fitted between a primary link and its adjacent auxiliary link. No spring has to be installed across the spatial manipulator from a far remote link to ground such that the motion interference among the springs and the links can be prevented. Besides, since the embedded auxiliary links along the primary links of the manipulator form a series of spatial parallelogram revolute-spherical-spherical-revolute modules, the active DOFs of the system remain the same as the primary manipulator and the range of motion of the manipulator will not be hindered. As a result, the n-DOF manipulator can serve the general function of an articulated serial-type manipulator in kinematics. The simulated results of a 6DOF gravity-balanced manipulator modeled on ADAMS shows that the static equilibrium as well as the kinematics of the system can be successfully accomplished by this proposed methodology. [DOI: 10.1115/1.4001816]

1 Introduction

A mechanism is perfectly gravity balanced if the considered system is in static equilibrium at all configurations, i.e., the gravity effects are completely eliminated from the system of interest [1,2]. For robotic manipulators, gravity balance of the system benefits from the improvement of input energy efficiency [3–6]. As a consequence, little or no external force is required to sustain the system payloads at any configuration or while slowly operated with a vertical movement. The gravity balance of a system can be achieved by various methods, e.g., the counterweight method, the linkage and cam mechanism method, and the spring suspension method [3]. With the advantage of having relatively small inertia, use of springs in balancing techniques is considered as a more efficient approach than others in the perspective of saving energy.

The simplest gravity-balanced mechanism is a spring-loaded, ground-pivoted pendulum [1,2]. By the installation of a zero-free-length spring, the full compensation of gravitational force of the pendulum by the spring force can be easily achieved at any position. Over the years, extensive studies on the designs of perfectly gravity-balanced planar mechanisms comprising of zero-free-length springs had been reported [7–10]. Various arrangements for the mechanical realization of zero-free-length springs, using conventional nonzero-free-length springs, have also been presented [7,11–13]. The ideally weight-negligible spring device can be realized by the use of cables, pulleys, and linear springs [14,15]. Some proposed a spring parameter optimization method to improve the balancing accuracy for normal spring installations [16].

One of the difficulties for the design of a spring balancing mechanism comes from the selection of the spring attachment points to generate an exact amount of forces or torques to counterbalance the gravity effects of the whole mechanism during motions. Passive auxiliary links are usually used to trace the center of gravity and to provide proper attachment points for fitted springs. Nevertheless, while the spring balancing techniques are applied to a spatial mechanism, e.g., a manipulator, the arrangement of auxiliary links and springs becomes complicated and cumbersome. Although numerous gravity-balanced designs of spatial serial-type mechanisms have been proposed [12,17–22], most of them are only applicable to specific applications due to the limited degrees of freedom (DOFs) or the restricted orientations of the joint axes of the mechanisms. Designs of spring-loaded gravity-balanced spatial manipulator with the ability to serve a general spatial motion are few. Recently, Agrawal and Fattah [19] proposed a methodology for the gravity balance of a general spatial manipulator by the use of pantograph-alike, parallel, auxiliary links along with the zero-free-length springs to compensate the gravitational forces of the system. However, the arrangement of auxiliary links and springs is rather complicated, especially for high-DOF mechanisms. As reported in their study, a 3DOF spatial manipulator requires five zero-free-length springs where one of the springs has to be fitted between the base and the mass center of the system. Because of this, possible motion interference among the auxiliary links, the attached springs, and the manipulator itself may interpose the range of motion of the manipulator.

In this paper, a novel methodology for the design of a spring-loaded gravity-balanced spatial manipulator is developed, where the static equilibrium condition is derived based on the potential energy method. The overall gravitational potential energy of n serially connected links is formulated as sum of n independent subsystems where each subsystem is considered in pure rotation in space. Extended from the balancing technique of the well-known single-link equilibrator where the spring is attached between ground and the rotating link, a concept of a pseudobase on each of the n subsystems is thus developed. Since the n pseudobases travel in space along with their associated links, n consecutive modules of spatial parallelogram revolute-spherical-spherical-revolute (RSSR) linkage are constructed to provide a pseudobase for each subsystem. With the attachment of a zero-free-length spring to a primary link and its adjacent pseudobase link, the gravity-balanced design of the n-DOF spatial manipulator can be accomplished. In this proposed methodology, no spring has to be installed across a number of primary links from a remote link to ground and, hence, the motion interference among the manipula-

[1]Paper presented in part at the ASME 2009 Design Engineering Technical Conference (DETC2009), San Diego, CA, Aug. 30–Sep. 2, 2009 (DETC2009-87170).

[2]Corresponding author.

Contributed by the Mechanisms and Robotics Committee of ASME for publication in the JOURNAL OF MECHANISMS AND ROBOTICS. Manuscript received January 5, 2010; final manuscript received April 29, 2010; published online June 21, 2010. Assoc. Editor: Delun Wang.

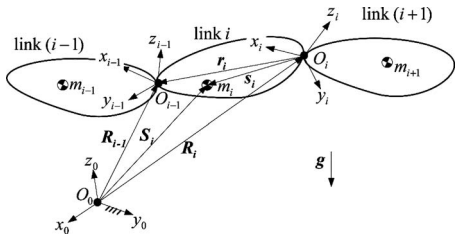

Fig. 1 A segment of the *n* serially connected links

tor, auxiliary links, and springs can be largely reduced. The simulated results of a 6DOF gravity-balanced spatial manipulator as an industrial manipulator are presented in support of the proposed methodology.

2 Formulation of the Gravitational Potential Energy of a Manipulator Into That of *n* Rotational Subsystems

Consider n serially connected links, as shown in Fig. 1, where all links are post- and preconnected with a revolute joint. Let frame 0 be fixed on ground at point O_0 and frame i fixed on link i at point O_i, where O_i is on the axis of the revolute joint connecting links i and $(i+1)$. The gravitational potential energy of link i can be expressed as

$$U_{g,i} = -m_i \boldsymbol{g} \cdot \boldsymbol{S_i} = -m_i \boldsymbol{g} \cdot (\boldsymbol{R_i} + \boldsymbol{s_i}) \tag{1}$$

where the pointing-downward vector $\boldsymbol{g}$ is the gravity vector, m_i is the mass of link i, and $\boldsymbol{R_i}$ is the position vector of point O_i from O_0. Vectors $\boldsymbol{S_i}$ and $\boldsymbol{s_i}$ are the position vectors of the mass center of link i from points O_0 and O_i, respectively.

Referring to Fig. 1,

$$\boldsymbol{R_i} = \boldsymbol{R_{i-1}} - \boldsymbol{r_i} \tag{2}$$

where $\boldsymbol{r_i}$, pointing from points O_i to O_{i-1}, is referred to the link vector of link i.

Writing Eq. (2) j times for $j=1,\ldots,i$ and summing the j recursive equations, Eq. (2) can be rewritten as

$$\boldsymbol{R_i} = -\sum_{j=1}^{i} \boldsymbol{r_j} \tag{3}$$

Substituting Eq. (3) into Eq. (1) yields

$$U_{g,i} = -m_i \boldsymbol{g} \cdot \left(\boldsymbol{s_i} - \sum_{j=1}^{i} \boldsymbol{r_j} \right) \tag{4}$$

The total gravitational potential energy of the n serially connected links can be obtained by summing Eq. (4) for each link i and rearranging the right-hand-side terms of Eq. (4) as

$$\sum_{i=1}^{n} U_{g,i} = -\boldsymbol{g} \cdot \sum_{i=1}^{n} \left(m_i \boldsymbol{s_i} - \sum_{j=i}^{n} m_j \boldsymbol{r_i} \right) \tag{5}$$

Equation (5) can be further expressed in a condensed form as

$$\sum_{i=1}^{n} U_{g,i} = -\sum_{i=1}^{n} \mu_i \boldsymbol{g} \cdot \boldsymbol{\sigma_i} \tag{6}$$

where

$$\mu_i = m_i + \sum_{j=i}^{n} m_j \tag{7}$$

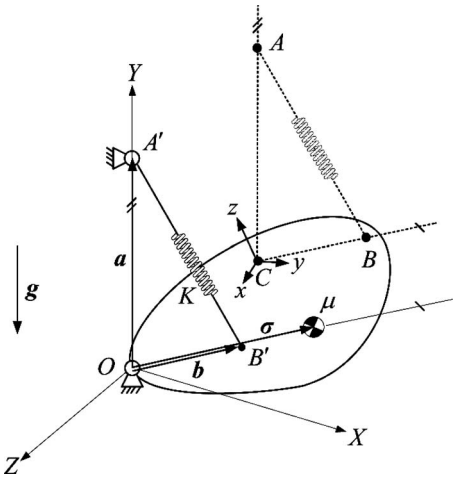

Fig. 2 Gravity balance of a rigid body mounted on ground with a single spring

$$\boldsymbol{\sigma_i} = \frac{m_i \boldsymbol{s_i} - \sum_{j=i}^{n} m_j \boldsymbol{r_i}}{m_i + \sum_{j=i}^{n} m_j} \tag{8}$$

The gravitational potential energy of the n serially connected links in Eq. (6) can be considered as sum of the gravitational potential energy of n subsystems, where each subsystem contributes the gravitational potential energy of $(-\mu_i \boldsymbol{g} . \boldsymbol{\sigma_i})$, for $i = 1,2\ldots,n$, to the system, respectively. As indicated in Eq. (7), each subsystem possesses the mass of link i and the accumulated mass of link i through link n. Since vectors $\boldsymbol{s_i}$ and $\boldsymbol{r_i}$ are both fixed on link i, vector $\boldsymbol{\sigma_i}$ of Eq. (8) is also fixed on link i. This indicates that vector $\boldsymbol{\sigma_i}$ is only dependent on the orientation of link i with respect to the inertia frame and is irrelevant to the absolute position of link i. Hence, the gravitational potential energy of each subsystem i is equivalent to that of a pure-rotation link, with the mass of μ_i and with $\boldsymbol{\sigma_i}$ as its position vector of mass center, which resembles to a single-link equilibrator, as shown in Fig. 2. This, in turn, implies that static equilibrium condition of each subsystem can be possibly obtained if each spring of the system is desired to be installed locally.

3 The Single-Link Equilibrator and the Pseudobases of *n*-DOF Manipulator

Consider the single-link equilibrator comprised of a link with the mass of μ mounted on ground with a spherical joint and a zero-free-length spring fitted between ground and the link, as illustrated in Fig. 2. The static balance of such an equilibrator is well known and justified [23,24]. At any configuration, the overall potential energy, namely, the sum of elastic potential energy and the gravitational potential, is constant as

$$\frac{1}{2} K (\boldsymbol{b} - \boldsymbol{a})^2 - \mu \boldsymbol{g} \cdot \boldsymbol{\sigma} = \text{const} \tag{9a}$$

or

$$-K \boldsymbol{b} \cdot \boldsymbol{a} + \tfrac{1}{2} K (a^2 + b^2) - \mu \boldsymbol{g} \cdot \boldsymbol{\sigma} = \text{const} \tag{9b}$$

where $\boldsymbol{a}$ and $\boldsymbol{b}$, respectively, are the position vectors from spherical joint O to point A' on ground and point B' on the link, $\boldsymbol{\sigma}$ is the position vector of mass center of the link, and K is the spring constant.

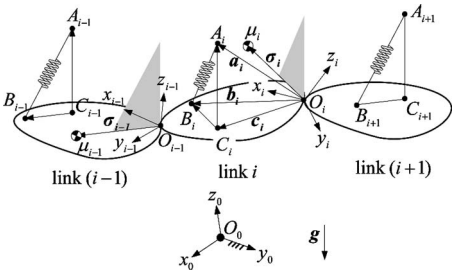

Fig. 3 Spring triangle $A_iB_iC_i$ for each link i

Since the angle between vectors $\boldsymbol{a}$ and $\boldsymbol{b}$ and the angle between vectors $\boldsymbol{g}$ and $\boldsymbol{\sigma}$ are both dependent to the rotation of the link, if the variable terms $(K\boldsymbol{a}\cdot\boldsymbol{b})$ and $(-\mu\boldsymbol{g}\cdot\boldsymbol{\sigma})$ in Eq. (9*b*) are always equal as

$$K\boldsymbol{a}\cdot\boldsymbol{b} = -\mu\boldsymbol{g}\cdot\boldsymbol{\sigma} \tag{10}$$

Then, Eq. (9*b*) can be satisfied at any configuration of the link. Equation (10) is thus a sufficient condition of Eq. (9*b*) and is the equilibrium condition of the single-link equilibrator. In order to satisfy the condition of Eq. (10), one of the easiest arrangements is to install a spring at the attachment points with OA' parallel to the direction of gravity and OB' parallel to the position vector of the mass center. With such arrangement, spring constant K and the magnitudes of $\boldsymbol{a}$ and $\boldsymbol{b}$ can be readily selected according to Eq. (10). Once the spring attachment points A' and B' are determined, a spring triangle $A'B'O$ is formed. In general, as shown in Fig. 2, any spring attachment points A and B forming a spring triangle ABC congruent and parallel to $A'B'O$ guarantee the same spring deflected length AB and the equilibrium condition of the system remains satisfied.

According to Eq. (6), the gravitational potential energy of subsystem i can be considered equivalently as a rigid body mounted on ground with the mass of μ_i and with $\boldsymbol{\sigma_i}$ as its position vector of mass center. The gravitational potential energy of subsystem i can be expressed as

$$\Upsilon_{g,i} = -\mu_i\boldsymbol{g}\cdot\boldsymbol{\sigma_i} \tag{11}$$

On an arbitrary point C_i of link i, a zero-free-length spring of stiffness K_i is attached with a spring triangle $A_iB_iC_i$, as shown in Fig. 3. The elastic potential energy of spring K_i can be expressed as

$$U_{s,i} = \tfrac{1}{2}K_i[(\boldsymbol{b_i}-\boldsymbol{c_i})-(\boldsymbol{a_i}-\boldsymbol{c_i})]^2 = -K_i(\boldsymbol{a_i}-\boldsymbol{c_i})\cdot(\boldsymbol{b_i}-\boldsymbol{c_i}) + \tfrac{1}{2}K_i(l_{CA,i}^2 + l_{CB,i}^2) \tag{12}$$

where $l_{CA,i}$ and $l_{CB,i}$ are the magnitudes of vectors $(\boldsymbol{a_i}-\boldsymbol{c_i})$ and $(\boldsymbol{b_i}-\boldsymbol{c_i})$, respectively.

Let lines C_iA_i and C_iB_i be parallel to the gravity vector and the mass center position vector $\boldsymbol{\sigma_i}$, respectively. Vectors $(\boldsymbol{a_i}-\boldsymbol{c_i})$ and $(\boldsymbol{b_i}-\boldsymbol{c_i})$ can then be obtained as

$$\boldsymbol{a_i}-\boldsymbol{c_i} = -\frac{l_{CA,i}}{g}\boldsymbol{g} \tag{13}$$

$$\boldsymbol{b_i}-\boldsymbol{c_i} = \frac{l_{CB,i}}{\sigma_i}\boldsymbol{\sigma_i} \tag{14}$$

Substituting Eqs. (13) and (14) into Eq. (12) yields

$$U_{s,i} = \frac{K_i l_{CA,i} l_{CB,i}}{g\sigma_i}\boldsymbol{g}\cdot\boldsymbol{\sigma_i} + \frac{1}{2}K_i(l_{CA,i}^2 + l_{CB,i}^2) \tag{15}$$

For the gravitational potential energy of subsystem i to be balanced by the elastic potential energy of spring K_i, the sum of Eqs. (11) and (15) has to be constant. Thus, one sufficient equilibrium condition comprising of the following equations can be identified as

$$K_i l_{CA,i} l_{CB,i} = \mu_i g\sigma_i \tag{16}$$

$$l_{CA,i} = \text{const} \tag{17}$$

and

$$l_{CB,i} = \text{const} \tag{18}$$

Based on Eq. (16), the spring stiffness K_i and the spring installing lengths, $l_{CA,i}$ and $l_{CB,i}$, can be obtained, where any two of the design parameters, K_i, $l_{CA,i}$, and $l_{CB,i}$, can be determined arbitrarily. According to Eqs. (17) and (18), point B_i can be a fixed point on link i, while side C_iA_i is vertically lying on a rigid body jointed to link i at point C_i. The rigid body is referred to the pseudobase of link i, for its resemblance of the base, as shown in Fig. 2. For the balance of gravitational potential energy each subsystem i, n pseudobases are constructed along with the primary chain of link i, as shown in Fig. 4.

4 Realization of Pseudobases by Series of Spatial Parallelogram RSSR Modules

4.1 Kinematics of a Spatial Parallelogram RSSR Linkage. The kinematic requirement of a pseudobase is that the line drawn between the spring attachment point A_i and the spherical joint C_i always remains vertical regardless of the motion of link i. Such a parallel motion between the pseudobase and ground can be achieved by the application of a spatial parallelogram linkage. As shown in Fig. 5, an arbitrary spatial parallelogram RSSR linkage can be defined by the twist angle α and the constant lengths of PQ, QN, NO, OP, and QM. The features of the spatial parallelogram RSSR linkage are as follows: Axes of the revolute joints at P and M are parallel; points P, Q, and M are on the same plane;

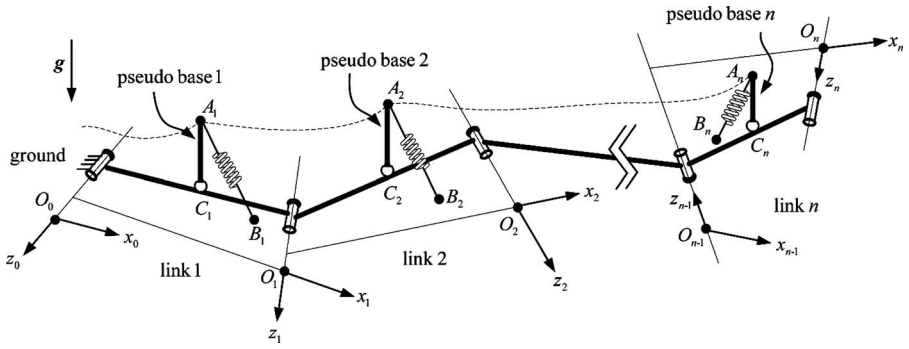

Fig. 4 Pseudobases and the attached springs

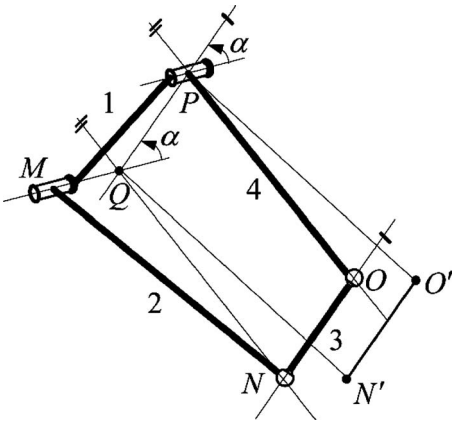

Fig. 5 A spatial parallelogram RSSR linkage

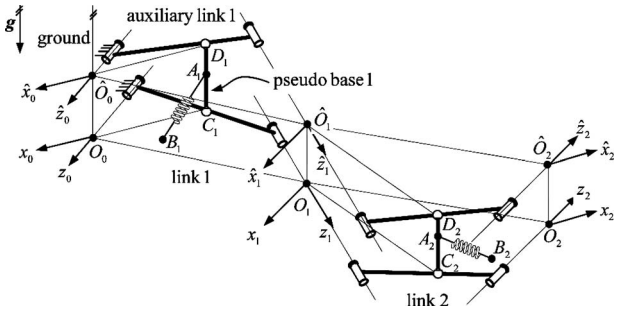

Fig. 6 Two consecutive RSSR linkages in series

lengths PQ and QN are equal to lengths NO and OP, respectively. By the mobility equation [25], a RSSR mechanism has one active DOF and one idle DOF [26] as

$$F = \lambda(n - j - 1) + \Sigma f_i = 6(4 - 4 - 1) + 2 \cdot 1 + 2 \cdot 3 = 2 \quad (19)$$

Due to the special geometrical arrangement of parallelogram $PQNO$, the active DOF allows links 2 and 4 rotating with the same angular velocity and line ON remains in parallel with line PQ at any configuration. The idle DOF allows link 3 to spin axially about the line passing through the two spherical joints O and N. Hence, if line PQ is in vertical direction with respect to a base, link 3 is a pseudobase with line ON remaining vertical at all times. Furthermore, the line jointing any two arbitrary points N' and O' on links 2 and 4, respectively, is also a vertical line if quadrilateral $PQN'O'$ is a parallelogram. This indicates that the positioning of link 3 is not uniquely located on link 2 as long as a parallelogram can be formed. It is important to note that, the parallelism of lines PQ, ON, and $O'N'$ holds for any configuration of the RSSR linkage. Once line PQ is constrained vertically, lines ON and $O'N'$ remain vertical as well. Since twist angle α is the angle between lines PQ and MQ, as the direction of joint axis MQ of the revolute joint at M changes, the twist angle α will also change. Link 2 of the floating RSSR linkage can be in a general spatial motion with three complete rotations as (i) rotation about axis MQ, (ii) rotation of twist angle α, namely, about an axis normal to the plane containing lines PQ and MQ, and (iii) rotation about axis PQ, and three complete translations as the free translations of line PQ. Conclusively, the additional links 1, 3, and 4 chained to link 2 do not constraint the motion of link 2.

4.2 Construction of Pseudobases by a Series of RSSR Modules Onto the Spatial Manipulator. Given any spatial, all-revolute, serial-type manipulator, the pseudobase for each primary link can be easily obtained by embedding a series of consecutive spatial parallelogram RSSR linkages onto the manipulator, as illustrated in Fig. 6. For the first auxiliary RSSR linkage, the rotation axis of the revolute joint connecting auxiliary link 1 and ground has to be parallel to that of the revolute joint connecting link 1 and ground and these two axes have to be in the same vertical plane, according to the features of the spatial RSSR parallelogram. With such arrangements, any vertical line $O_0\hat{O}_0$ that intersects both revolute axes can be found. By forming quadrilateral $O_0C_1D_1\hat{O}_0$ as a parallelogram, spherical joint C_1 on primary link 1 and spherical joint D_1 on auxiliary link 1 can be located. Similarly, by forming quadrilateral $O_0O_1\hat{O}_1\hat{O}_0$ as another parallelogram, the positions of points O_1 and $\hat{O}_1$ can also be obtained. As a result, both lines C_1D_1 and $O_1\hat{O}_1$ are vertical. Following the construction of the first RSSR linkage, the second module can be constructed based on the vertical line $O_1\hat{O}_1$ following the similar procedure. A spatial serial-type manipulator with n active DOFs can then be constructed with n consecutive RSSR modules. Since the entire system, including the primary and the auxiliary links, comprises $3n$ moving links, $2n$ revolute joints, and $2n$ spherical joints, the mobility of such a system can be calculated as

$$F = 6[(3n + 1) - 4n - 1] + (2n) \cdot 1 + (2n) \cdot 3 = 2n \quad (20)$$

Equation (20) indicates that, disregarding the n idle DOFs, the entire mechanism has n active DOFs, same as the primary manipulator. This also suggests that the auxiliary linkage does not add additional motion constraints to the original kinematic chain.

The spherical joints can be realized by ball joints or spherical mechanisms. However, a ball joint usually suffers from a limited range of rotation and induces a singular configuration, resulting in a limited range of motion of the mechanism. A singularity-free spherical joint had been proposed and can be applied [27].

5 Gravity Balance of the Spatial Manipulator

Referring to the spatial equilibrator, as shown in Fig. 7, the gravity effects due to the pseudobases and the auxiliary links can be considered as follows. Since the auxiliary links are connected serially along with the primary links of the manipulator, the total gravitational potential energy of the auxiliary links can be derived in a similar form as that of Eq. (5) as

$$\sum_{i=1}^{n} \hat{U}_{g,i} = -\boldsymbol{g} \cdot \sum_{i=1}^{n} \left(\hat{m}_i \hat{\boldsymbol{s}}_i - \sum_{j=i}^{n} \hat{m}_j \hat{\boldsymbol{r}}_i \right) \quad (21)$$

where $\hat{m}_i$ is the mass of auxiliary link i, $\hat{\boldsymbol{s}}_i$ and $\hat{\boldsymbol{r}}_i$ are the position vectors of the mass center, and the link vector of auxiliary link i referenced from origin $\hat{O}_i$ of frame $\hat{i}$, respectively.

The gravitational potential energy of the pseudobase i is

$$U^*_{g,i} = -m^*_i \boldsymbol{g} \cdot (\boldsymbol{R}_i + \boldsymbol{c}_i + \boldsymbol{s}^*_i) \quad (22)$$

where m^*_i is the mass of pseudobase i, $\boldsymbol{c}_i$ is the position vector of point C_i referenced from origin O_i, and $\boldsymbol{s}^*_i$ is the position vector of the mass center of pseudobase i referenced from the spherical joint C_i.

Since line C_iD_i is parallel to the gravity vector, the inner product of the gravity vector and vector $\boldsymbol{s}^*_i$ is constant. Substituting Eq. (3) in Eq. (22) yields

$$\sum_{i=1}^{n} U^*_{g,i} = -\boldsymbol{g} \cdot \sum_{i=1}^{n} \left(m^*_i \boldsymbol{c}_i - \sum_{j=i}^{n} m^*_j \boldsymbol{r}_i \right) + \text{const} \quad (23)$$

By summing Eqs. (5), (21), and (23), the overall gravitational potential energy of the spatial equilibrator in Fig. 7 can be rewritten in a condensed form as that of Eq. (6) where the combined mass and its position vector can be modified from Eqs. (7) and (8), respectively, as

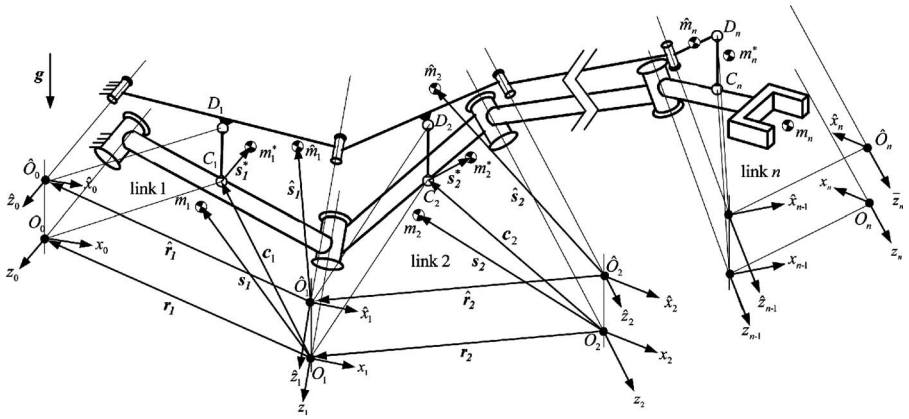

Fig. 7 The general *n*-DOF spatial manipulator

$$\tilde{\mu}_i = m_i + \hat{m}_i + m_i^* + \sum_{j=i}^{n} (m_j + \hat{m}_j + m_j^*) \tag{24}$$

$$\tilde{\boldsymbol{\sigma}}_i = \frac{m_i \boldsymbol{s}_i + \hat{m}_i \hat{\boldsymbol{s}}_i + m_i^* \boldsymbol{c}_i + \sum_{j=i}^{n} (-m_j \boldsymbol{r}_i - \hat{m}_j \hat{\boldsymbol{r}}_i - m_j^* \boldsymbol{r}_i)}{m_i + \hat{m}_i + m_i^* + \sum_{j=i}^{n} (m_j + \hat{m}_j + m_j^*)} \tag{25}$$

With Eqs. (24) and (25), the positions of the n combined mass centers can be identified on each primary link of the spatial manipulator. Vectors $\boldsymbol{s_i}$, $\boldsymbol{c_i}$, and $\boldsymbol{r_i}$ referenced from origin O_i can be represented by constant coordinates of frame i. Since frames i and $\hat{i}$ are the coordinate systems fixed, respectively, on primary link i and auxiliary link i and these two coordinate systems are always in parallel, coordinates of frames $\hat{i}$ can be easily transformed by an identity matrix to coordinates of frame i. Hence, vectors $\hat{\boldsymbol{s}}_i$, $\hat{\boldsymbol{r}}_i$ and the combined mass center position vector $\tilde{\boldsymbol{\sigma}}_i$ can be represented by constant coordinates of frame i. Thus, by replacing μ_i and $\boldsymbol{\sigma}_i$ of Eq. (16) with the modified parameters $\tilde{\mu}_i$ and $\tilde{\boldsymbol{\sigma}}_i$, the balancing conditions of the spatial manipulator can be obtained with the spring stiffness and the spring installing lengths, for each link i.

6 A Simulated Model of a 6DOF Gravity-Balanced Manipulator

Figure 8 shows a 6DOF, six-link industrial manipulator with all-revolute joints. Since the axis of the first joint between ground and link 1 is in the direction of gravity, the total gravitational potential energy induced by the rotation of link 1 about the first joint axis does not change. Hence, the problem for the gravity balance of the considered manipulator is simplified to obtain the static equilibrium of the remaining five links. As shown in Fig. 8, five pseudobases and five auxiliary links are added to the system. Although the simulation model shown may have motion interferences at certain postures, an actual embodiment of a system without interference is possible if links are properly shaped. Since each pair of the auxiliary link and the primary link has identical direction of rotation, their instantaneous working planes, which are normal to the instantaneous rotation axes, can be parallel. Frames i and $\hat{i}$ are, respectively, attached to link i and auxiliary link i for $i=0,1,2,\ldots,6$. The Denavit–Hartenberg (DH) parameters [28] of the manipulator for frames i and $\hat{i}$ are listed in Table 1, respectively.

The mass properties and the link geometries required for Eqs. (24) and (25) are listed in Table 2. The link vectors of link i and auxiliary link i, the mass center position vectors of link i, the auxiliary link i, and the position vectors of the center of spherical joint on link i are all expressed in coordinates with respect to frame i and shown in Table 2. The accumulated point mass $\tilde{\mu}_i$ and its position vector $\tilde{\boldsymbol{\sigma}}_i$ of subsystem i are evaluated according to Eqs. (24) and (25) and also tabulated in Table 2. According to Eq. (16), two spring design parameters K_i and $l_{CA,i}$ are selected before $l_{CB,i}$ is determined. The values of the spring parameters and the coordinates of the spring attachment points, A_i and B_i of each spring, with respect to frame i are derived from Eqs. (13) and (14) and listed as the $\boldsymbol{a_i}$ and $\boldsymbol{b_i}$ in Table 3.

The manipulator, along with the pseudobases and auxiliary links, are modeled in the simulation software ADAMS with a specified motion given as follows: the angular displacement function for each joint i with respect to time is defined as

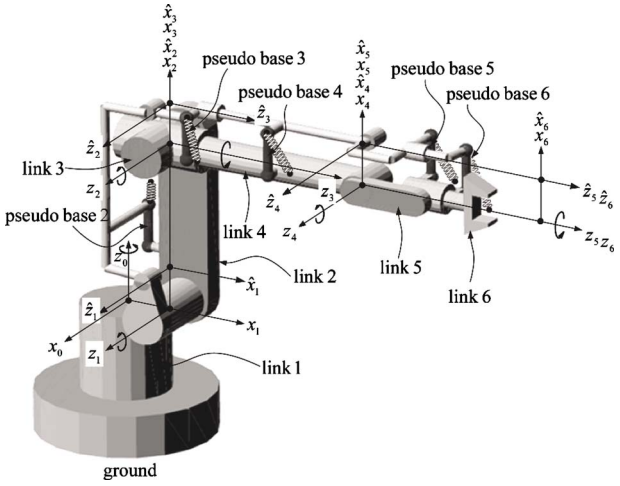

Fig. 8 A 6DOF gravity-balanced manipulator

Table 1 DH parameters for the manipulator (data given in m)

Frame $i/\hat{i}$	$d_i/\hat{d}_i$	$\theta_i/\hat{\theta}_i$	$a_i/\hat{a}_i$	$\alpha_i/\hat{\alpha}_i$ (deg)
$1/\hat{1}$	0/0.1	θ_1	0.1/0.1	90/90
$2/\hat{2}$	0/0	θ_2	0.4/0.4	0/0
$3/\hat{3}$	0/0	θ_3	0/0	90/90
$4/\hat{4}$	0.5/0.5	θ_4	0/0	−90/−90
$5/\hat{5}$	0/0	θ_5	0/0	90/90
$6/\hat{6}$	0.27/0.27	θ_6	0/0	0/0

Table 2 Parameters of mass and geometry properties (data given in kg and m)

Link i	2	3	4	5	6
m_i	23.21	24.51	15.13	6.12	2.20
m_i^*	0.47	0.47	0.47	0.47	0.47
$\hat{m}_i$	2.38	0.81	1.58	1.32	0.27
$\boldsymbol{s}_i$	(−0.20, 0.00, −0.1)	(0, 0, 0)	(0, 0.16, 0.00)	(0, 0.02, 0.11)	(0, 0.00, −0.02)
$\hat{\boldsymbol{s}}_i$	(−0.17, 0.07, 0.06)	(0, 0.02, 0.10)	(0, 0.13, 0.00)	(0, 0.01, 0.09)	(0, −0.02, −0.08)
$\boldsymbol{r}_i$	(−0.4, 0, 0)	(0, 0, 0)	(0, 0.5, 0)	(0, 0, 0)	(0, 0, −0.27)
$\hat{\boldsymbol{r}}_i$	(−0.4, 0, 0)	(0, 0, 0)	(0, 0.5, 0)	(0, 0, 0)	(0, 0, −0.27)
$\boldsymbol{c}_i$	(−0.3, 0.1, −0.1)	(0, 0.06, 0.09)	(0, 0.21, 0.06)	(0, −0.1, 0.1)	(0, −0.06, −0.06)
$\tilde{\mu}_i$	105.92	79.59	45.21	18.76	5.88
$\tilde{\boldsymbol{\sigma}}_i$	(0.25, 0.00, −0.02)	(0, 0.00, 0.00)	(0, −0.25, 0.00)	(0, 0.00, 0.05)	(0, −0.01, 0.12)

Table 3 Spring design parameters

Spring i	K_i (kN/m)	$l_{CA,i}$ (m)	$l_{CB,i}$ (m)	$\boldsymbol{a}_i$ (m)	$\boldsymbol{b}_i$ (m)
2	20.0	0.1	0.13	(−0.2, 0.1, −0.1)	(−0.17, 0.10, −0.11)
3	2.0	0.08	0.01	(0.08, 0.06, 0.09)	(0, 0.06, 0.09)
4	15.0	0.08	0.09	(0.08, 0.21, 0.06)	(0, 0.12, 0.06)
5	2.0	0.08	0.05	(0.08, −0.1, 0.1)	(0, −0.09, 0.15)
6	1.0	0.08	0.09	(0.08, −0.06, −0.06)	(0, −0.06, 0.03)

Table 4 Coefficients of the joint displacement function

Joint i	t_I	t_F	θ_I	θ_F	a_0	a_1	a_2	a_3
1	0	5	1.57	−0.42	1.57	0.0000	−0.2388	0.0318
2	0	5	1.57	0.57	1.57	0.0000	−0.12	0.016
3	0	5	0	1	0	0	0.12	−0.016
4	1	3	0	1	1	−2.25	1.5	−0.25
5	5	9	0	1.2	10.3125	−5.0625	0.7875	−0.0375
6	5	9	0	2.5	21.4844	−10.5429	1.6406	−0.0781

$$\theta_i(t) = \begin{cases} 0 \le t < t_I, & \theta_I \\ t_I \le t < t_F, & a_0 + a_1 t + a_2 t^2 + a_3 t^3 \\ t_F \le t < 10, & \theta_F \end{cases} \tag{26}$$

where θ_I and θ_F are the initial and final values of the actuated joint angles θ_i at time t_I and t_F, respectively.

From t_I to t_F, a cubic polynomial function is assumed for the angular displacement of each joint. The units for the angular displacement and time are given in radian and seconds, respectively. The coefficients of the cubic polynomials of Eq. (26) for each joint i are listed in Table 4.

Figure 9 shows the results of the simulated motion described in

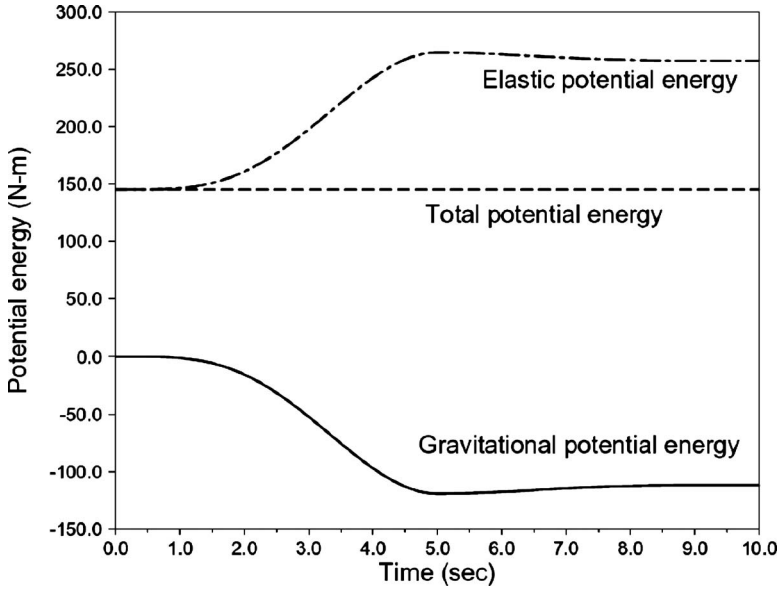

Fig. 9 Variations of potential energies

Eq. (26). The total potential energy of the system remained constant throughout the entire range of motion of the industrial manipulator, where the elastic potential energy function is a reflection of the gravitational potential energy function. As a result, the gravity effect of the system is fully eliminated and a perfect gravity balance of the system is accomplished.

7 Conclusion

In this paper, a methodology for the design of a gravity-balanced general spatial serial-type manipulator is presented. The static equilibrium of the system is derived based on the potential energy method. The overall gravitational potential energy of n serially connected links is successfully formulated into n independent subsystems. By generalization of the basic single-link equilibrator, the equilibrium of each subsystem is achieved with the suspension of a zero-free-length spring fitted between each primary link and its adjacent pseudobase link. Construction of the n pseudobase links is implemented by the use of the n consecutive modules of spatial parallelogram RSSR linkages. The proposed design method outperforms others because only n springs are required, all springs are fitted locally, and the mobility of the original manipulator remains intact. Thus, the motion interference among the springs, the auxiliary links, and the manipulator is minimized and, since the range of motion is not scarified, the gravity-balanced manipulator is able to serve a more general spatial motion in comparison with others. Verification of the methodology concerning the static equilibriums as well as kinematics is justified by the computer simulation of an example.

References

[1] Nathan, R. H., 1985, "A Constant Force Generation Mechanism," ASME J. Mech., Transm., Autom. Des., **107**(4), pp. 508–512.

[2] Streit, D. A., and Gilmore, B. J., 1989, "'Perfect' Equilibrators for Rotatable Bodies," ASME J. Mech., Transm., Autom. Des., **111**(4), pp. 451–458.

[3] Baradat, C., Arakelian, V., Briot, S., and Guegan, S., 2008, "Design and Prototyping of a New Balancing Mechanism for Spatial Parallel Manipulators," ASME J. Mech. Des., **130**(7), p. 072305.

[4] Gosselin, C. M., and Wang, J., 1998, "On the Design of Gravity-Compensated Six-Degree-of-Freedom Parallel Mechanisms," Proceedings of the 1998 IEEE International Conference on Robotics and Automation, Leuven, Beigium, May.

[5] Gosselin, C. M., 1999, "Static Balancing of Spherical 3-DOF Parallel Mechanisms and Manipulators," Int. J. Robot. Res., **18**(8), pp. 819–829.

[6] Herder, J. L., 1998, "Design of Spring Force Compensation Systems," Mech. Mach. Theory, **33**, pp. 151–161.

[7] Streit, D. A., and Shin, E., 1993, "Equilibrators for Planar Linkages," ASME J. Mech. Des., **115**(3), pp. 604–611.

[8] Lin, P.-Y., Shieh, W.-B., and Chen, D.-Z., 2009, "Design of Perfectly Static-Balanced One-DOF Planar Linkage With Revolute Joint Only," ASME J. Mech. Des., **131**(5), pp. 051004.

[9] Laliberte, T., Gosselin, C. M., and Martin, J., 1999, "Static Balancing of 3-DOF Parallel Mechanism," IEEE/ASME Trans. Mechatron., **4**(4), pp. 363–377.

[10] Wongratanaphisan, T., Cole, M. O. T., 2008, "Analysis of a Gravity Compensated Four-Bar Linkage Mechanism With Linear Spring Suspension," ASME J. Mech. Des., **130**(1), p. 011006.

[11] Van Dorsser, W. D., Herder, J. L., Wisse, B. M., and Barents, R., 2008, "Balancing device," U.S. Patent No. 0,210,842-A1.

[12] Rahman, T., Ramanathan, R., Seliktar, R., and Harwin, W., 1995, "A Simple Technique to Passively Gravity-Balance Articulated Mechanisms," ASME J. Mech. Des., **117**(4), pp. 655–658.

[13] Van Dorsser, W. D., Barents, R., Wisse, B. M., Schenk, M., and Herder, J. L., 2008, "Energy-Free Adjustment of Gravity Equilibrators by Adjusting the Spring Stiffness," Proc. Inst. Mech. Eng., Part C: J. Mech. Eng. Sci., **222**(9), pp. 1839–1846.

[14] Tuda, G., and Mizuguchi, O., 1983, "Arm With Gravity-Balancing Function," U.S. Patent No. 4,383,455.

[15] Ebert-Uphoff, I., and Johnson, K., 2002, "Practical Considerations for the Static Balancing of Mechanisms of Parallel Architecture," Proc. Inst. Mech. Eng., Part K: J. Multi-body Dynamics, **216**, pp. 73–85.

[16] Arakelian, V., and Ghazaryan, S., 2008, "Improvement of Balancing Accuracy of Robotic Systems: Application to Leg Orthosis for Rehabilitation Devices," Mech. Mach. Theory, **43**(5), pp. 565–575.

[17] Wongratanaphisan, T., and Chew, M., 2002, "Gravity Compensation of Spatial Two-DOF Serial Manipulators," J. Rob. Syst., **19**(7), pp. 329–347.

[18] Tuijthof, G. J. M., and Herder, J. L., 2000, "Design, Actuation and Control of an Anthropomorphic Robot Arm," Mech. Mach. Theory, **35**(7), pp. 945–962.

[19] Agrawal, S. K., and Fattah, A., 2004, "Gravity-Balancing of Spatial Robotic Manipulator," Mech. Mach. Theory, **39**(12), pp. 1331–1344.

[20] Brown, G., and DiGuilio, A. O., 1980, "Support Apparatus," U.S. Patent No. 4,208,028.

[21] Simionescu, I., and Ciupitu, L., 2000, "The Static Balancing of the Industrial Robot Arms Part I: Discrete Balancing," Mech. Mach. Theory, **35**, pp. 1287–1298.

[22] Simionescu, I., and Ciupitu, L., 2000, "The Static Balancing of the Industrial Robot Arms Part II: Continuous Balancing," Mech. Mach. Theory, **35**, pp. 1299–1311.

[23] Gosselin, C. M., 2006, "Adaptive Robotic Mechanical Systems: A Design Paradigm," ASME J. Mech. Des., **128**(1), pp. 192–198.

[24] Arsenault, M., and Gosselin, C. M., 2007, "Static Balancing of Tensegrity Mechanisms," ASME J. Mech. Des., **129**(3), pp. 295–300.

[25] Kutzbach, K., 1929, "Mechanische Leitengsverzweigung, Maschinenbau," Der Betrieb, **8**(21), pp. 710–716.

[26] Waldron, K. J., and Kinzel, G. L., 1999, *Kinematics, Dynamics, and Design of Machinery*, Wiley, New York, pp. 22–25.

[27] Arikawa, K., 2008, "Realization of a 6-DOF Manipulator With an Unconventional Topological Structure," ASME Paper No. DETC2008-49621.

[28] Denavit, J., and Hartenberg, R. S., 1955, "A Kinematic Notation for Lower Pair Mechanisms Based on Matrices," ASME J. Appl. Mech., **77**, pp. 215–221.